APPLIED ORGANOMETALLIC CHEMISTRY
Appl. Organometal. Chem. 2001; **15**: 581–592
DOI: 10.1002/aoc.199

Computational study of dimethyl- and trimethyl-tin(IV) complexes of porphyrin derivatives

Dario Duca,[1,2]* Giampaolo Barone,[1] Gianfranco La Manna,[3] Tiziana Fiore,[1] Claudia Pellerito,[2] Roberta Di Stefano,[2] Michelangelo Scopelliti[2] and Lorenzo Pellerito[2]

[1]Dipartimento di Scienze Farmaceutiche, Università degli Studi di Salerno, Via Ponte don Melillo, 84084 Fisciano (SA), Italy
[2]Dipartimento di Chimica Inorganica, Università degli studi di Palermo, Viale delle Scienze, 90128 Palermo, Italy
[3]Dipartimento di Chimica Fisica, Università degli studi di Palermo, Viale delle Scienze, 90128 Palermo, Italy

The molecular geometry, energetics and electronic charge distribution of diorgano- and triorgano-tin(IV) complexes of [protoporphyrin-IX] and [*meso*-tetra(4-carboxyphenyl)porphine] derivatives were determined at semi-empirical and *ab initio* levels. To study the molecular details of the complexes, simpler molecule models were calculated by the *ab initio* pseudo-potential method. The molecular properties of these complexes are essentially independent of the presence of the peripheral tin atoms. Agreement was always found among the results of the different computational approaches, as well as between the theoretical and the experimental findings on the molecular geometry of the hypothesized complexes. Interaction modes between water and the organo-tin systems considered were affected strongly by the presence of peripheral tin atoms. Copyright © 2001 John Wiley & Sons, Ltd.

Keywords: organotin(IV)–porphyrin complexes; semi-empirical method; pseudo-potential method, computational study

Received 7 July 2000; accepted 28 November 2000

INTRODUCTION

A series of papers concerning the synthesis, the structural characterization and the biological activity of diorgano- and triorgano-tin(IV) complexes with the peripheral donor groups of [protoporphyrin-IX] (H_4PPIX),[1,2] [*meso*-tetra(4-carboxyphenyl)porphine] and [*meso*-tetra(4-sulfonatophenyl)porphine], H_6TPPC[3–5] and H_6TPPS,[6] have recently appeared in the literature. These studies have stimulated further work, still in progress, on diorgano- and triorgano-tin(IV) complexes with some derivatives of the ligands above. These derivatives, [$SnCl_2$–protoporphyrin-IX] (H_2SnCl_2PPIX), [$SnCl_2$–*meso*-tetra(4-carboxyphenyl)porphine] (H_4SnCl_2TPPC) and [$SnCl_2$–*meso*-tetra(4-sulfonatophenyl)porphine] (H_4SnCl_2TPPS), differ from H_4PPIX, H_6TPPC and H_6TPPS by having an $SnCl_2$ group centered perpendicularly to the porphyrin ring.

Usually, organotin(IV) compounds interact strongly with biological substrates, very often giving rise to toxic effects.[7] This has to be carefully considered because, owing to their industrial applications,[8] organotin(IV) compounds are widespread in the environment.[9]

It has been shown, both by experimental[10,11] and/or computational[12] studies, that methyltin(IV) moieties have a small affinity to the nitrogen bases with respect to the phosphate groups of DNA. These latter interactions would not seem able to induce substantial modifications to the DNA and hence could not explain the dramatic toxicity of the tin(IV) moieties. However, it is known that diorgano- and triorgano-tin(IV) compounds make

---

* Correspondence to: D. Duca, Dipartimento di Scienze Farmaceutiche, Università degli Studi di Salerno, Via Ponte don Melillo, 84084 Fisciano (SA), Italy.
Email: dduca@unisa.it

Contract/grant sponsor: Italian Ministero dell'Università e della Ricerca Scientifica e Tecnologica (M.U.R.S.T.).
Contract/grant sponsor: University of Salerno.
Contract/grant sponsor: University of Palermo.

stable complexes with biological ligands[13,14] containing oxygen, sulfur and nitrogen donor atoms and, it is likely that the observed biological activity of the organotin(IV) compounds could be modulated by the presence of these ligands.

In this paper we attempt to rationalize, by theoretical computations, experimental findings on the molecular geometry and energetics of the complexes between dimethyl- and trimethyl-tin(IV) moieties with the biologically significant H_4PPIX, H_6TPPC, H_2SnCl_2PPIX and H_4SnCl_2TPPC ligands. A comparison between these species, having peripheral carboxylic groups, and H_6TPPS and H_4SnCl_2TPPS species, having peripheral sulfonic groups, is also performed. The presence of molecules of water was explicitly taken into consideration, to account for the observed solid-state structures and to hypothesize possible changes of these structures in water media.

In the following, we will generally refer to H_4PPIX, H_6TPPC, H_6TPPS and H_2SnCl_2PPIX, H_4SnCl_2TPPC, H_4SnCl_2TPPS as porphyrin and tin–porphyrin ligands respectively.

COMPUTATIONAL METHODS

The SCF semi-empirical PM3 method[15,16] and the LANL2DZ[17–19] pseudo-potential method were employed to obtain geometrical parameters and Mulliken charge distributions. The LANL2DZ[17–19] pseudo-potential method was also used to calculate electrostatic potential[20] maps and to study simplified model systems. The GAUSSIAN98W package[21] was employed on a PC Pentium III (600 MHz) to perform the calculations.

The PM3 method was employed to optimize the geometry of the porphyrin ligands H_4PPIX, H_6TPPC, H_6TPPS, of the tin–porphyrin ligands H_2SnCl_2PPIX, H_4SnCl_2TPPC, H_4SnCl_2TPPS, and of their dimethyl- and trimethyl-tin(IV) complexes. Owing to the peculiarity of the systems studied (see below), and to simplify the discussion of the results, we mainly considered the dimethyl- and trimethyl-tin(IV) complexes, hydrated or non-hydrated, of H_6TPPC and H_4SnCl_2TPPC: $(Me_2Sn)_nH_{6-n}TPPC$, $(Me_3Sn)_nH_{6-n}TPPC$, $(Me_2Sn)_nH_{4-n}SnCl_2TPPC$ and $(Me_3Sn)_nH_{4-n}SnCl_2TPPC$, n being in the range 1–4.

Within the notation (Me_2Sn) is always included an $HCOO^-$ group, which counterbalances the residual charge of the dimethyltin(IV) fragment linked by a carboxylic group to a porphyrin or tin–porphyrin ligand. Since $HCOO^-$ groups mimic porphyrin molecules, in $(Me_2Sn)_nH_{6-n}TPPC$ and $(Me_2Sn)_nH_{4-n}SnCl_2TPPC$ species the peripheral tin atoms of (Me_2Sn) fragments represent polymerization centers while two porphyrin molecules are bound to any of them.

To obtain more information on the geometry and atomic charge of species around the peripheral tin atoms, the HF/LANL2DZ method was employed to optimize simplified models of the $(Me_mSn)_nH_{6-n}TPPC$ and $(Me_mSn)_nH_{4-n}SnCl_2TPPC$ systems, m being 2 or 3. Atomic charge distribution was evaluated through the Mulliken population analysis on the optimized structures, at the PM3 and LANL2DZ level. The values of the Mulliken charge on the tin atoms, q_{Sn}, were related to the experimental ^{119}Sn Mössbauer isomer shift, δ, parameters.[22]

RESULTS AND DISCUSSION

Optimized structural parameters of porphyrin and tin–porphyrin ligands are reported in Table 1. The starting geometrical parameters, when available,[23–25] were taken from X-ray data tables. The optimized structure of H_4SnCl_2TPPC is shown in

Table 1 Structural parameters calculated by the PM3 method

	H_4PPIX	H_2SnCl_2PPIX	H_6TPPC	H_4SnCl_2TPPC	H_6TPPS	H_4SnCl_2TPPS
N—N—N—N[a] (°)	4.2	0.0	3.7	0.0	3.7	0.0
N—N[b] (nm)	0.419	0.416	0.413	0.414	0.413	0.417
ClSnCl (°)	–	180.0	–	179.7	–	179.7
Cl—Cl (nm)	–	0.482	–	0.482	–	0.481

[a] Dihedral angle defined by the nitrogen atoms in the porphyrin moiety. Experimental (X-ray) values in similar system were 3.8°[23] and 0.3°[24]

[b] Distance between N(pyrrole)—N(pyrrole) non-neighbor atoms. Analogous experimental (X-ray) parameters in similar systems were 0.404 nm,[23] 0.406 nm[24] and more significantly for tin compounds 0.421 nm.[25]

Scheme 1 as an example of the tin–porphyrin systems studied here.

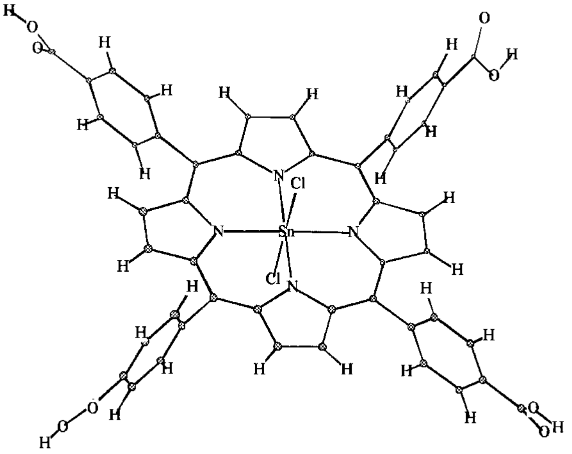

H_4SnCl_2TPPC

Scheme 1

The analysis of Table 1 shows that:

- the tin moiety inserted in the porphyrin center removes the small folding angle present in the porphyrin ring;
- the geometry of the tin moieties bound by different tin porphyrin ligands is not affected when changing the ligands.

Furthermore, the analysis of the optimized parameters of the species $(Me_3Sn)H_3SnCl_2TPPC$, $(Me_3Sn)_2H_2SnCl_2TPPC$ and $(Me_3Sn)_4SnCl_2TPPC$ showed that, irrespective of the number of peripheral tin fragments, the value of the distances N(pyrrole)—N(pyrrole) (non-neighbor N atoms) and Cl—Cl are 0.414 nm and 0.482 nm respectively, whereas the value of the dihedral angle defined by the four nitrogen atoms of the porphyrin center N—N—N—N is equal to 0 °. This value shows that the porphyrin plane is not folded by the introduction of peripheral trimethyltin(IV) fragments. Moreover, since the angle ClSnCl is, in any of the $(Me_3Sn)_nH_{4-n}SnCl_2TPPC$ species, equal to 180.0 ± 0.3 ° and the ClSnN angles 90.0 ± 0.5 °, the octahedral arrangement of the central tin atom is not distorted by the peripheral modifications of the tin–porphyrin ligands.

In Table 2, the angles involved in the arrangement of the peripheral tin atoms determined at the PM3 level for $(Me_3Sn)H_3SnCl_2TPPC$ and at the HF/LANL2DZ level for $Me_3Sn(HCOO)$ are reported. For the former and the latter species the same parameters are also reported at the same levels, when they are coordinated by one water molecule. The introduction of water molecules, considered as interacting with the peripheral tin centers and, therefore, placed in their coordination sphere, was suggested by experimental findings[26] showing up to six molecules of water coordinated to $(Me_3Sn)_4SnCl_2TPPC$ species in the solid state. The peripheral tin fragments, hydrated or non-hydrated, are reported in Scheme 2.

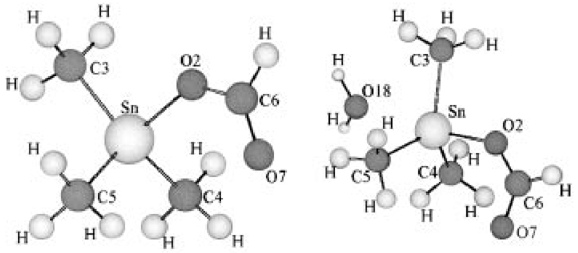

$Me_3Sn(HCOO)$ $Me_3Sn(HCOO)\cdot H_2O$

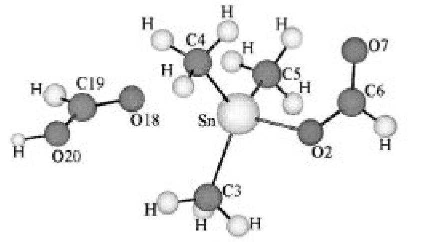

$Me_3Sn(HCOO)\cdot HCOOH$

Scheme 2

The coordination distance Sn—O between the carboxylate oxygen of the $HCOO^-$ group and the tin atom, Sn—$O_{carboxy}$, and the distance between the tin atom and the oxygen of the water molecule, Sn—O_{water}, are reported in Table 2.

The analysis of Table 2 points out the following:

- non-hydrated peripheral tin atoms have a distorted tetrahedral arrangement. This is observed at the PM3 level for the peripheral tin of the $(Me_3Sn)_nH_{4-n}SnCl_2TPPC$ species and at the HF/LANL2DZ level for the model $Me_3Sn(HCOO)$ species;
- the distortion of the peripheral tin environment is increased by the introduction of a coordinating molecule of water;
- as expected, the distortion due to the introduction of the water molecules is in the direction of a trigonal bi-pyramidal (tbp) arrangement. In fact, the values of the CSnC angles are around 120 °, whereas the OSnO angles (oxygen

Table 2 Bond angles and Sn—O interatomic distances[a] involving the peripheral tin atoms

	O_2SnC_3 (°)	O_2SnC_4 (°)	O_2SnC_5 (°)	C_3SnC_4 (°)	C_3SnC_5 (°)	C_4SnC_5 (°)	Sn—$O_{carboxy}$ (nm)	Sn—O_{water} (nm)
$(Me_3Sn)H_3SnCl_2TPPC$	96.5	112.4	112.4	114.4	109.9	109.9	0.203	–
$Me_3Sn(HCOO)$	101.0	106.1	106.1	114.0	114.0	113.9	0.198	–
$(Me_3Sn)H_3SnCl_2TPPC{\cdot}H_2O$	94.6	107.7	107.7	118.4	112.7	112.7	0.203	0.279
$Me_3Sn(HCOO){\cdot}H_2O$	95.8	101.0	99.9	118.5	117.1	117.4	0.202	0.265

[a] For the meaning of the labels refer to Scheme 2 in which the optimized structure of $Me_3Sn(HCOO){\cdot}H_2O$ and $Me_3Sn(HCOO)$ are reported: in this scheme it is possible to individualize the atoms involved in the different angles for the model molecules. The angles of $(Me_3Sn)H_3SnCl_2TPPC$, hydrated and non-hydrated, molecules were related to the same notation.

atoms, from the water molecule and the carboxylate group) are close to 180 ° (not reported in Table 2);

- both $(Me_3Sn)_nH_{4-n}SnCl_2TPPC$ and $Me_3Sn(HCOO)$ species show the same behavior when a coordinating water molecule is included in the system: increasing and decreasing the CSnC and OSnC angles respectively and leaving almost unchanged the $Sn—O_{carboxy}$ distance;
- $Me_3Sn(HCOO)$ species are suitable models of the interactions occurring by the carboxylate groups of the tin porphyrin ligands with trimethyltin(IV) moieties;
- the PM3 method, for the systems reported, reaches conclusions in qualitative agreement with the HF/LANL2DZ method.

In Scheme 2 the optimized (HF/LANL2DZ) adduct between the species $Me_3Sn(HCOO)$ and HCOOH is also reported. Formic acid molecules were employed like models of $(Me_3Sn)_nH_{4-n}SnCl_2TPPC$ species; hence they mimicked polymerization branches occurring via Sn—O interactions. The formic acid molecule induced in the $Me_3Sn(HCOO)$ species a distortion similar to that produced by the water molecules. However, the Sn—O distance between the tin and the HCOOH oxygen atom was 30% longer than the already discussed $Sn—O_{water}$ distance (Table 2). So, we judge as unlikely polymerization occurring via peripheral tin atoms of both $(Me_3Sn)_4SnCl_2TPPC$ and $(Me_3Sn)_4H_2TPPC$ complexes, because it would involve a large steric hindrance and a non-favorable Sn—O interaction distance.

The study of the species $(Me_3Sn)_nH_{6-n}TPPC$ allows one to understand the mutual effects between the tin atoms of the porphyrin ring and the peripheral fragments. The OSnC and CSnC angles, and the $Sn—O_{carboxy}$ distance of the latter in the $(Me_3Sn)_nH_{6-n}TPPC$ species for a given n, were identical to those of $(Me_3Sn)_nH_{4-n}SnCl_2TPPC$ species. Moreover, the N—N—N—N dihedral angle and the N(pyrrole)—N(pyrrole) distance in the porphyrin ring of the $(Me_3Sn)_nH_{6-n}TPPC$ and of the H_6TPPC species were almost unchanged. Therefore, the characteristics of the peripheral tin atoms in these porphyrin and tin–porphyrin derivatives, as observed experimentally,[26] do not affect the structure of the porphyrin ring whether complexed or not with the $SnCl_2$ moiety.

We studied the peripheral fragments of $(Me_2Sn)_nH_{4-n}SnCl_2TPPC$ by considering the $Me_2Sn(HCOO)_2$ species. As before, the HCOOH and $HCOO^-$ groups were introduced to mimic porphyrin species. In Scheme 3 the optimized (HF/LANL2DZ) geometry of $Me_2Sn(HCOO)_2$ (CI) and $Me_2Sn(HCOO)_2·HCOOH$ (CII, CIII) species are reported.

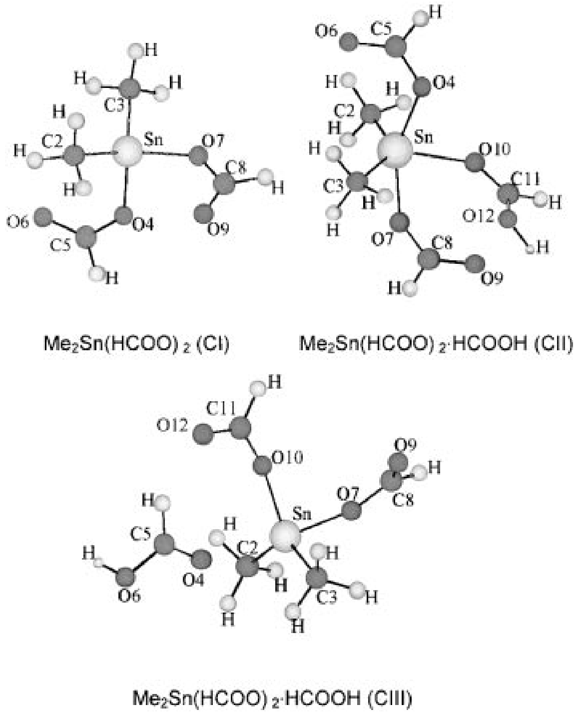

Me₂Sn(HCOO)₂ (CI) Me₂Sn(HCOO)₂·HCOOH (CII)

Me₂Sn(HCOO)₂·HCOOH (CIII)

Scheme 3

The CII is 34.9 kJ mol^{-1} less stable than the CIII isomer. The coordination energy, determined by considering the counter-poise correction because of the basis set superposition error (BSSE),[27] between the tetrahedral $Me_2Sn(HCOO)_2$ and the molecule of formic acid involved in forming the less stable CII conformer was 16.4 kJ mol^{-1}. Therefore, in the presence of formic acid molecules, a distorted tbp geometry, typical of the CII and CIII conformers, is energetically more stable than a tetrahedral geometry. This could also suggest that the tin atoms of the peripheral dimethyltin(IV) fragments in the porphyrin and tin–porphyrin complexes should act as a multi-polymerization center. Indeed, in this case, since porphyrins cannot act as bidentate ligands (minimum distance between the oxygen atoms of the two carboxylic groups was ~1.4 nm), the CII and CIII models mimic polymerization processes occurring by the involvement of three porphyrin units per tin atom.

Another possible cause of distortion in the tetrahedral arrangement of $Me_2Sn(HCOO)_2$ could be the presence of water molecules embodied in the structure of the peripheral dimethyltin(IV) fragments.[26] Scheme 4 shows the structures of the hydrated $Me_2Sn(HCOO)_2$ species optimized at the HF/LANL2DZ level.

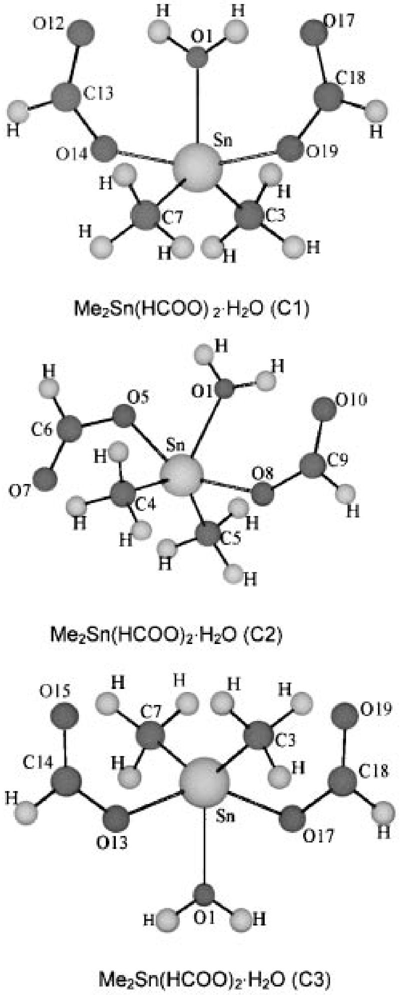

$Me_2Sn(HCOO)_2 \cdot H_2O$ (C1)

$Me_2Sn(HCOO)_2 \cdot H_2O$ (C2)

$Me_2Sn(HCOO)_2 \cdot H_2O$ (C3)

Scheme 4

C1 is energetically more stable (29 kJ mol^{-1}) than the C2 and C3 conformers. In all of the three species, the two $HCOO^-$ groups lie together with the tin atom and the water molecule on the same plane. We believe that the formation of hydrogen bonding between the hydrogen atoms of the molecule of water and the oxygen atoms of the HCOO—Sn(IV) fragments could determine the observed energetic stability of the conformers. The coordination energy ΔE, between the tetrahedral species CI and one water molecule involved to arrange the most stable C1 conformer, was calculated by considering the BSSE[27] correction. The value $\Delta E = -105.7$ kJ mol^{-1} shows that, in the presence of water, the tbp geometry of the C1–C3 conformers, and hence of the peripheral dimethyltin(IV) moieties of the porphyrin and tin–porphyrin complexes, is energetically more stable than the tetrahedral geometry. The ΔE value also shows that the hydrated C1–C3 species are energetically more stable than the CII and CIII conformers. Therefore, taking into account the unfavorable steric hindrance effects certainly present in systems where three porphyrin units are placed close to one another, we think that only the hydrated peripheral tin atoms, i.e. the C1–C3 arrangements, act as polymerization centers in dimethyltin(IV) complexes of porphyrin and tin–porphyrin ligands.

Hydrated and non-hydrated $(Me_2Sn)_nH_{4-n}SnCl_2TPPC$ species were optimized at the PM3 level. Porphyrin centers of $(Me_2Sn)_nH_{4-n}SnCl_2TPPC$, $(Me_3Sn)_nH_{4-n}SnCl_2TPPC$ and of H_4SnCl_2TPPC species showed identical geometric characteristics. Therefore, the $Me_2Sn(IV)$ peripheral moieties (as already observed for $Me_3Sn(IV)$) do not induce geometrical changes in the octahedral tin complexed by the four N(pyrrole) atoms of the porphyrin ring.

The structural parameters of the conformer C1 and of the hydrated and non-hydrated $(Me_2Sn)_4SnCl_2TPPC$ complex are reported in Table 3.

In Tables 4a and b are reported the Mulliken charges, determined at HF/LANL2DZ and PM3 levels, of selected atoms of dimethyl- and trimethyl-tin(IV) complexes and models of the porphyrin and tin-porphyrin ligands. Tables 4a and b show the following:

- identical values of the atomic charge are obtained for homologous atoms in the complexes and models;
- a slight difference between the charge of the peripheral and the pyrrolic tin is observed. There is also a small difference in the tin charge of the dimethyl- and the trimethyltin(IV) fragments, and in the peripheral tin, whether coordinated or not with molecules of water;
- effects on the nitrogen pyrrolic atoms caused by the presence of different peripheral tin and/

Table 3 Structural parameters of $Me_2Sn(HCOO)_2{\cdot}H_2O$,[a] C1 conformer, and of the hydrated and non-hydrated $(Me_2Sn)_4SnCl_2TPPC$[b] complexes

	O_1SnC_3[c] (°)	C_3SnC_7[c] (°)	OSnO[d] (°)	OHHO[e] (°)	SnO_{water}[f] (nm)	HO[g] (nm)
$Me_2Sn(HCOO)_2{\cdot}H_2O$ (C1)	115.3	129.4	160.3	0.0	0.208	0.171
$(Me_2Sn)_4SnCl_2TPPC{\cdot}4H_2O$	120.6	121.4	159.7	0.8	0.208	0.172
$(Me_2Sn)_4SnCl_2TPPC$	–	112.6	125.8	–	–	–

[a] Calculated at the HF/LANL2DZ level.

[b] Calculated at the PM3 level.

[c] See Scheme 4 to individualize elements, their serial numbers and the relative angle.

[d] Angle OSnO. O are the oxygen coordinating atoms of the carboxylate fragments (see Scheme 4).

[e] Dihedral angle formed by the two hydrogen atoms of the water molecule and the carboxylic oxygen atoms of the carboxylate fragments (see Scheme 4).

[f] Sn—O distance, the oxygen atom O being of the water molecule.

[g] The shortest HO distance, taken between one hydrogen atom of the water molecule and its closest carboxylate oxygen atom.

or coordinating groups, carboxylic or sulfonic, are *not* observed. Therefore, there is no reciprocal influence between peripheral and pyrrolic tin atoms;

- increasing negative charge is observed on pyrrolic nitrogen and carboxylic oxygen atoms that are coordinated to tin atoms;
- increasing positive charge on the tin peripheral center is observed with its coordination number.

Since analogous results are obtained when dimethyl- and trimethyl-tin(IV) complexes of the H_4PPIX an H_2SnCl_2PPIX ligands are considered, for the systems discussed the peripheral carboxylic groups have a behavior that can be considered as not depending on the porphyrin units.

It is possible to correlate the calculated Mulliken charge on the tin atoms, q_{Sn}, with the experimental ^{119}Sn Mössbauer isomer shift, δ, parameter.[26,28] The values of such parameters are related to the electron density on the tin atoms and show an inverse trend with their atomic charge.[22] In the species studied, for both ligands and complexes the δ values of the tin inserted into the pyrrolic ring are almost constant and, on average, are equal to 0.22 ± 0.04 mm s^{-1}.[26,28] Consistently, at the HF/LANL2DZ level, we found for these atoms a constant value of the Mulliken charge equal to 1.8 (see Table 4a). On the contrary, δ values[26,28] of the peripheral tin atoms of $(Me_2Sn)_4SnCl_2TPPC$, $(Me_2Sn)_4H_2TPPC$, $(Me_3Sn)_4SnCl_2TPPC$ and $(Me_3Sn)_4H_2TPPC$ species are equal to 1.00 ± 0.05 mm s^{-1}, 1.20 ± 0.05 mm s^{-1}, 1.25 ± 0.05 mm s^{-1} and 1.33 ± 0.05 mm s^{-1} respectively.

$(Me_2Sn)_4SnCl_2TPPC$ and $(Me_3Sn)_4SnCl_2TPPC$, in contrast with the $(Me_2Sn)_4H_2TPPC$ and $(Me_3Sn)_4H_2TPPC$ species, presented some water molecules[26] in the solid state. It is to be stressed that experimental findings do not show water molecules located close to the $SnCl_2$ moiety. In fact, not one of the tin–porphyrin ligands, H_2SnCl_2PPIX, H_2SnCl_2TPPC or H_4SnCl_2TPPS, showed water molecules.[26] Therefore, it can be supposed that water mainly coordinates peripheral tin atoms.

Figure 1 shows the plot of the Mulliken charges of the tin atoms in the dimethyl- and trimethyl-tin(IV) fragments *versus* the experimental δ[26,28] of

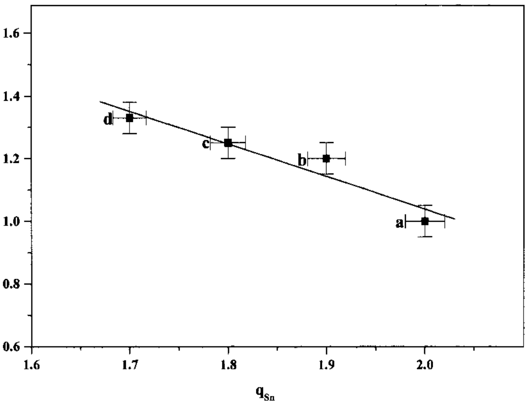

Figure 1 Isomer shifts, δ, versus tin Mulliken charge, q_{Sn}, of the peripheral tin in dimethyl- and trimethyl-tin(IV) complexes of porphyrin and tin–porphyrin ligands. A value of $q_{Sn} = 2.0$ was found in $Me_2Sn(HCOO)_2{\cdot}HCOOH$, CII–CIII models, and $Me_2Sn(HCOO)_2{\cdot}H_2O$, C1–C3 models, 1.9 and 1.8 in $Me_2Sn(HCOO)_2$, CI model, and $Me_3Sn(HCOO){\cdot}H_2O$, and 1.7 in $Me_3Sn(HCOO){\cdot}HCOOH$ and $Me_3Sn(HCOO)$. Solid line is the least-squares fit, weighted by the experimental error values, of data points (■). The error bars are reported taking into account the experimental error on δ and considering an error of 1% on the values of the calculated q_{Sn}.

Table 4a Mulliken charges (u.a.) on some atoms of ligands and of their dimethyl- and trimethyl-tin(IV) complexes determined at the HF/LANL2DZ\|PM3 levels

	$Sn_{(p)}$[a]	$Sn_{(c)}$[b]	Cl[c]	N_H[d]	N[e]	$O_{(C)Sn}$[f]	$O_{(C)}$[g]	$O_{(f)Sn}$[h]	$O_{(f)}$[i]	$O_{(water)}$[j]	$C_{(Me)}$[k]
H_4PPIX	–	–	–	−0.7|0.3	−0.4|−0.2	–	–	–	–	–	–
H_6TPPS	–	–	–	−0.7|0.3	−0.4|−0.2	–	–	–	–	–	–
H_6TPPC	–	–	–	−0.7|0.3	−0.4|−0.2	−0.4|−0.4[l]	−0.6|−0.3	–	–	–	–
H_2SnCl_2PPIX	–	1.8|2.0	−0.5|−0.7	–	−0.9|−0.2	–	–	–	–	–	–
H_4SnCl_2TPPS	–	1.8|2.0	−0.5|−0.7	–	−0.9|−0.2	–	–	–	–	–	–
H_4SnCl_2TPPC	–	1.8|2.0	−0.5|−0.7	–	−0.9|−0.2	−0.4|−0.4[l]	−0.6|−0.3	–	–	–	–
$(Me_3Sn)_4H_2$TPPC	1.7|1.6	–	–	−0.7|0.3	−0.4|−0.2	−0.8|−0.6	−0.5|−0.5	–	–	–	−1.0|−0.8
$(Me_3Sn)_4SnCl_2$TPPC	1.7|1.6	1.8|2.0	−0.5|−0.7	–	−0.9|−0.2	−0.8|−0.6	−0.5|−0.5	–	–	–	−1.0|−0.8
$(Me_3Sn)_4H_2TPPC\cdot 4H_2O$	1.8|1.6	–	–	−0.7|0.3	−0.4|−0.2	−0.8|−0.6	−0.5|−0.5	–	–	−0.8|−0.4	−1.0|−0.8
$(Me_3Sn)_4SnCl_2TPPC\cdot 4H_2O$	1.8|1.6	1.8|2.0	−0.5|−0.7	–	−0.9|−0.2	−0.8|−0.6	−0.5|−0.5	–	–	−0.8|−0.4	−1.0|−0.8
$(Me_2Sn)_4H_2$TPPC	1.9|1.9	–	–	−0.7|0.3	−0.4|−0.2	−0.8|−0.6	−0.6|−0.5	−0.8|−0.6	−0.5|−0.5	–	−1.0|−0.8
$(Me_2Sn)_4SnCl_2$TPPC	1.9|1.9	1.8|2.0	−0.5|−0.7	–	−0.9|−0.2	−0.8|−0.6	−0.6|−0.5	−0.8|−0.6	−0.5|−0.5	–	−1.0|−0.8
$(Me_2Sn)_4H_2TPPC\cdot 4H_2O$	2.0|2.0	–	–	−0.7|0.3	−0.4|−0.2	−0.8|−0.7	−0.6|−0.5	−0.8|−0.7	−0.5|−0.5	−1.0|−0.5	−1.0|−0.8
$(Me_2Sn)_4SnCl_2TPPC\cdot 4H_2O$	2.0|2.0	1.8|2.0	−0.5|−0.7	–	−0.9|−0.2	−0.8|−0.7	−0.6|−0.5	−0.8|−0.7	−0.5|−0.5	−1.0|−0.5	−1.0|−0.8

Selected atoms: [a]peripheral tin, [b]pyrrole ring tin, [c]chlorine, averaged values of hydrogenated pyrrole nitrogen[d] and pyrrole nitrogen[e], [f]carboxylate coordinating oxygen bound or non-bound[l] to tin, [g]carboxylate uncoordinating oxygen, formate oxygen bound[h] and not bound[i] to tin, [j]oxygen of coordinated water molecule, [k]carbon of methyl in the methyltin(IV) moieties. For details, see Scheme 1 and text.

Table 4b Mulliken charges (u.a.) on some atoms of dimethyl- and trimethyl-tin(IV) peripheral models determined at the HF/LANL2DZ\|PM3 levels

	$Sn_{(p)}$[a]	$O_{(f)Sn}$[h]	$O_{(f)}$[i]	$O_{(water)}$[j]	$C_{(Me)}$[k]	$O_{(Hf)Sn}$[m]	$O_{(Hf)}$[n]
$Me_3Sn(HCOO)$	1.7|n.d.	−0.8|n.d.	−0.4|n.d.	–	−1.0|n.d.	–	–
$Me_3Sn(HCOO)\cdot H_2O$	1.8|1.6	−0.8|−0.6	−0.5|−0.5	−0.8|−0.4	−1.0|−0.8	–	–
$Me_3Sn(HCOO)\cdot HCOOH$	1.7|n.d.	−0.8|n.d.	−0.5|n.d.	–	−1.0|n.d.	−0.4|n.d.	−0.6|n.d.
$Me_2Sn(HCOO)_2$ (CI)	1.9|n.d.	−0.8|n.d.	−0.4|n.d.	–	−1.0|n.d.	–	–
$Me_2Sn(HCOO)_2\cdot HCOOH$ (CII)	2.0|n.d.	−0.8|n.d.	−0.5|n.d.	–	−1.0|n.d.	−0.6|n.d.	−0.5|n.d.
$Me_2Sn(HCOO)_2\cdot HCOOH$ (CIII)	2.0|n.d.	−0.8|n.d.	−0.5|n.d.	–	−1.0|n.d.	−0.5|n.d.	−0.5|n.d.
$Me_2Sn(HCOO)_2\cdot H_2O$ (C1)	2.0|n.d.	−0.8|n.d.	−0.5|n.d.	−1.1|n.d.	−1.0|n.d.	–	–
$Me_2Sn(HCOO)_2\cdot H_2O$ (C2)	2.0|n.d.	−0.8|n.d.	−0.5|n.d.	−1.0|n.d.	−1.0|n.d.	–	–
$Me_2Sn(HCOO)_2\cdot H_2O$ (C3)	2.0|n.d.	−0.8|n.d.	−0.4|n.d.	−0.9|n.d.	−1.0|n.d.	–	–

Selected atoms: [a,h,i,j,k] for the attribution of the labels refer to Table 4a. [m] O atoms of formic acid, oxygen bound to tin. [n]O atoms of formic acid, oxygen not bound to tin. For details, see Schemes 2–4 and text.

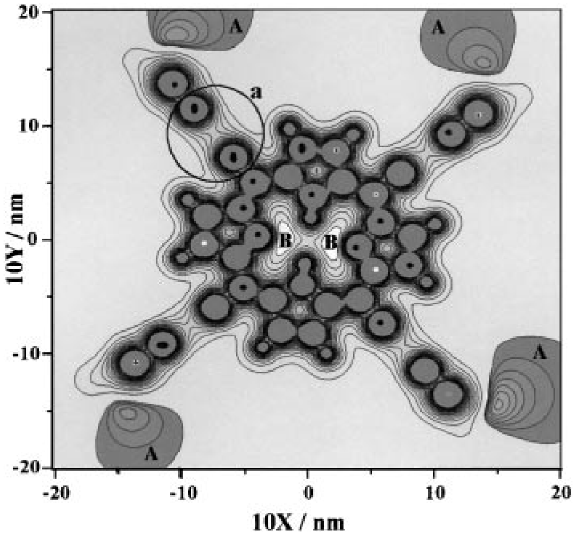

Figure 2 H_6TPPC ligand: projection onto the pyrrolic (*XY*) plane of the electrostatic potential function calculated at the HF/LANL2DZ level, *V*. In the gray-scale map the values of *V* are increasing with the gray tones. **A** and **B** regions are characterized by negative values of *V*; minima in the **A** and **B** areas are at −0.025 u.a. and −0.075 u.a. respectively. Iso-energetic lines in **A** show *V* increases of 0.004 u.a. The main region has positive *V* values in the range 0–1 u.a.; iso-energetic lines showing *V* increases of 0.05 u.a. Circle **a** locates one phenyl group of the porphyrin ligand.

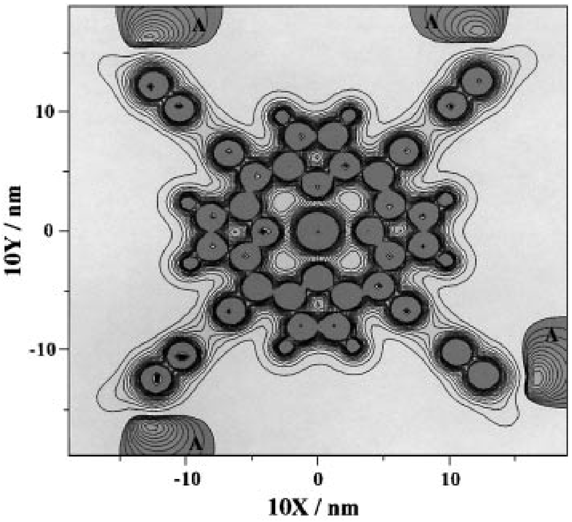

Figure 3 H_4SnCl_2TPPC ligand: projection onto the pyrrolic (*XY*) plane of *V*. Values of *V* are increasing with the gray tones. **A** areas with minima at −0.05 u.a. are characterized by just negative values of *V*. In the main region, *V* ranges between 0 and 1 u.a. values. Iso-energetic lines show *V* increases of 0.05 u.a. and 0.003 u.a. in the main and **A** regions respectively.

the peripheral tin atoms present in the complexes $(Me_2Sn)_4H_2TPPC$, $(Me_3Sn)_4H_2TPPC$, $(Me_2Sn)_4SnCl_2TPPC{\cdot}4H_2O$ and $(Me_3Sn)_4SnCl_2TPPC{\cdot}4H_2O$. In fact, the δ value of

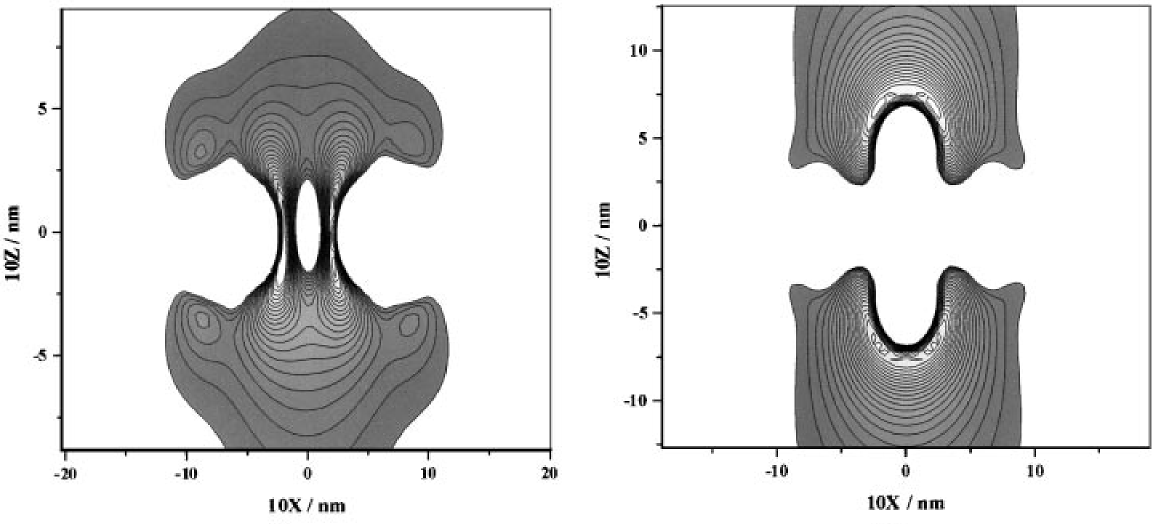

(i)

(ii)

Figure 4 H_6TPPC (i) and H_4SnCl_2TPPC (ii) ligands: projection on the *XZ* plane of *V*. White zone has *V* values above zero. Minima have values of −0.075 u.a.; iso-energetic lines show *V* increases of 0.004 u.a.

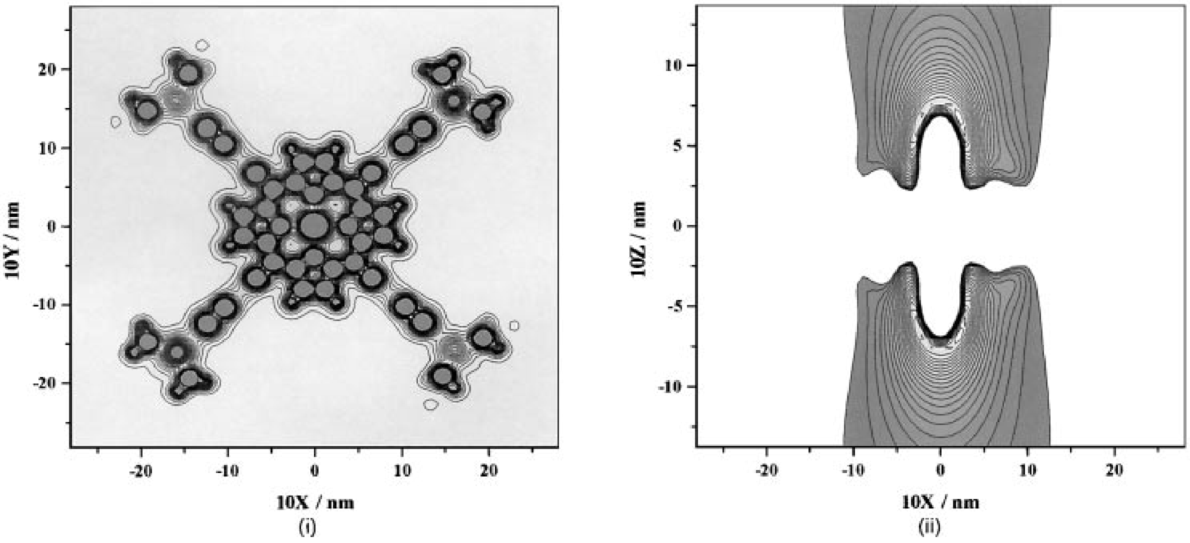

Figure 5 $(Me_3Sn)_4SnCl_2TPPC$ complex. (i) Projection onto the pyrrolic (*XY*) plane of *V*. *V* values, reported in the range 0–1 u.a., are increasing with the gray tones; the iso-energetic lines show *V* increases of 0.05 u.a. (ii) Projection onto the *XZ* plane of *V*. Minimum is at −0.075 u.a.; the iso-energetic lines show *V* increases of 0.004 u.a.; white zone has *V* values above zero.

the peripheral tin of the complexes above can be correlated to the q_{Sn} of dimethyl- and trimethyl-tin(IV) models characterized by analogous tin environments. The experimental δ of the peripheral tin of the hydrated $(Me_2Sn)_4SnCl_2TPPC$ complex could be caused by any of the environments of the C1–C3 models. Because of the energetics of the C1–C3 species, the value of the experimental δ found for $(Me_2Sn)_4SnCl_2TPPC$ should be mainly due to the tin atom environment of C1 (point **a**). The charge of the tetrahedral tin of $Me_2Sn(HCOO)_2$ and $Me_3Sn(HCOO)$ models should characterize the non-hydrated peripheral tin atoms of $(Me_2Sn)_4H_2TPPC$ and $(Me_3Sn)_4H_2TPPC$ complexes (points **b** and **d** respectively), whereas peripheral tin atoms of the hydrated $(Me_3Sn)_4SnCl_2TPPC$[26] should have the charge of $Me_3Sn(HCOO)\cdot H_2O$ model (point **c**). The trend between δ and q_{Sn} parameters of Fig. 1 has already been found in other organotin(IV) systems.[28,29]

Figures 2–7 show representations of the electrostatic potential distribution, *V*, of the H_6TPPC, H_4SnCl_2TPPC, $(Me_3Sn)_4SnCl_2TPPC$ and hydrated and non-hydrated $(Me_2Sn)_4SnCl_2TPPC$ species. In the figures, the point *V*(0, 0, 0) is set on the pyrrole ring center for H_6TPPC and on the pyrrole tin atom for all the other species. The figures show the projection of *V* onto the pyrrolic (*XY*) plane and onto the plane (*XZ*) perpendicular to the pyrrolic plane.

The figures clearly single out:

- the phenyl fragments placed perpendicular to the projection plane and the pyrrolic center, e.g. circle **a** on Fig. 2;
- the tin atoms, peripheral and coordinated to the pyrrole ring (Figs 3, 5–7).

Some carbon atoms of the coordinating porphyrin carboxylate and formate are also shown together with other carbon atoms of the methyl groups of the peripheral dimethyl- and trimethyl-tin(IV) fragments. Moreover, H_6TPPC (Figs 2 and 4(i)) shows a negative electrostatic potential area in the pyrrole center that is drastically modified by the introduction of the $SnCl_2$ fragment (Figs 3 and 4(ii)).

Figure 4(ii) and 5(ii), in a pictorial way, suggest that the introduction of peripheral trimethyl-tin(IV) fragments does not influence the properties of the central tin atoms. Of course, the same lack of influence was observed for the hydrated and non-hydrated dimethyl-tin(IV) fragments. As already pointed out, the carboxylic groups in the H_6TPPC and H_4SnCl_2TPPC ligands have very similar features, (Figs 2 and 3). However, the electrostatic potential properties of the carboxylic groups are strongly modified by peripheral tin species (Figs 5–7), whereas the region showing negative values of electrostatic potential around the carboxylic groups are present even after hydration of the peripheral tin (Figs 6 and 7).

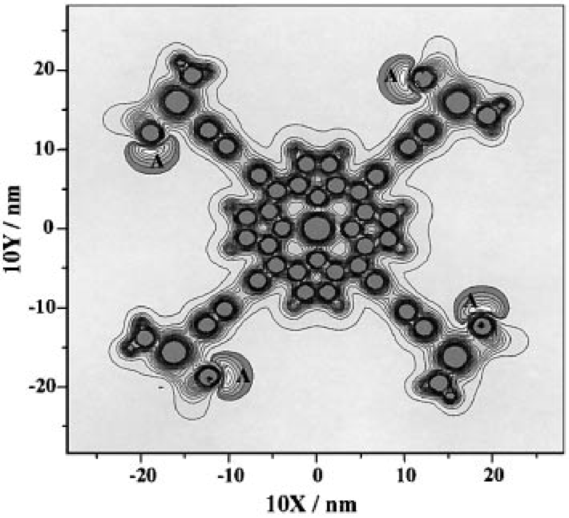

Figure 6 $(Me_2Sn)_4SnCl_2TPPC$ complex: projection onto the pyrrolic (*XY*) plane of *V*. Values of *V* are increasing with the gray tones. In the main region *V* has values ranging between 0 and 1 u.a.; iso-energetic lines show *V* increases of 0.05 u.a. **A** areas are characterized by just negative values of *V* with minima at −0.1 u.a. and iso-energetic lines showing *V* increases of 0.01 u.a.

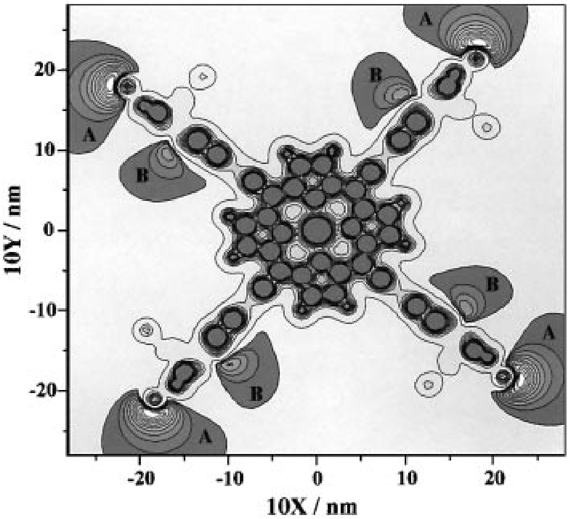

Figure 7 $(Me_2Sn)_4SnCl_2TPPC{\cdot}4H2O$ complex: projection onto the pyrrolic (*XY*) plane of *V*. Values of *V* are increasing with the gray tones. The central region has *V* values ranging between 0 and 1 u.a. and iso-energetic lines showing *V* increases of 0.05 u.a. **A** and **B** regions are characterized by just negative values of *V* with minima at −0.1 u.a. and −0.075 u.a. respectively; iso-energetic lines show *V* increases of 0.01 u.a.

As a consequence of this, the species represented in Figs 2–7 can interact with polar units, such as water, hence suggesting the possibility of existence of the same species in water media.

CONCLUSIONS

This work shows that theoretical and experimental data for the systems studied are in good agreement, hence allowing confidence in the derivation of results not achievable by experiments. Relevant findings are obtained on the systems studied by timely inexpensive semi-empirical methods and deeper information can be carried out at the *ab initio* level by simpler model systems.

In detail, our study mainly suggests that:

- the molecular properties (geometry, energetics and atomic charges) of the tin–porphyrin complex are not affected by the presence of peripheral tin atoms coordinated to the tin–porphyrin moieties;
- polymerization processes could likely occur in the diorganotin(IV) complexes of the porphyrin and tin–porphyrin ligands through the peripheral tin atoms acting as the polymerization centers;
- the presence of molecules of water gives rise to different interaction modes between these molecules and the peripheral tin atoms.

Acknowledgements Thanks are given to the Italian Ministero dell'Universitá e della Ricerca Scientifica e Tecnologica (M.U.R.S.T.), to the University of Salerno and to the University of Palermo for the financial support and to the University of Salerno for a fellowship to T.F. and G.B.

D.D. thanks Professor Francesco Maggio for his friendly constant support and helpful suggestions.

REFERENCES

1. Pellerito L, Pellerito A, Maggio F, Beltramini M, Salvato B, Ricchielli F. *Appl. Organomet. Chem.* 1993; **7**: 79.
2. Vitturi R, Catalano E, Lo Conte MR, Pellerito L. *Appl. Organomet. Chem.* 1993; **7**: 295.
3. Mirisola MG, Pellerito A, Fiore T, Stocco GC, Pellerito L, Cestelli A, Di Liegro I. *Appl. Organomet. Chem.* 1997; **11**: 499.
4. Triolo F, Pellerito C, Stocco GC, Fiore T, Maggio F, Pellerito L, Triolo R. *Appl. Organomet. Chem.* 1999; **13**: 733.

5. Mansueto C, Puccia E, Maggio F, Di Stefano R, Fiore T, Pellerito C, Triolo F, Pellerito L. *Appl. Organomet. Chem.* 2000; **14**: 189.
6. Pellerito A, Fiore T, Giuliani AM, Maggio F, Pellerito L, Mansueto C. *Appl. Organomet. Chem.* 1997; **11**: 707.
7. Arakawa Y. In *Chemistry of Tin*, Smith PJ (ed.). Blackie Academic & Professional: London, 1998; 388–428.
8. Evans CJ. In *Chemistry of Tin*, 2nd edn, Smith PJ (ed.). Blackie Academic & Professional, London, 1998; 442–479.
9. Champ MA, Seligman FP. *Organotin Enviromental Fate and Effects*. Chapman and Hall, London, 1997.
10. Barbieri R, Ruisi G, Silvestri A, Giuliani AM, Barbieri A, Spina G, Pieralli F, Del Giallo F. *J. Chem. Soc. Dalton Trans*. 1995; 467.
11. Barone G, Barbieri R, La Manna G, Koch MHJ. *Appl. Organomet. Chem.* 2000; **14**: 189.
12. Barone G, Barbieri R, Cotta Ramusino M, La Manna G. *J. Mol. Struct. (Theochem)* 1999; **469**: 143.
13. Silvestri A, Duca D, Huber F. *Appl. Organomet. Chem.* 1988; **2**: 417.
14. Gulì G, Gennaro G, Pellerito L, Stocco GC. *Appl. Organomet. Chem.* 1993; **7**: 407.
15. Stewart JJP. *J. Comp. Chem.* 1989; **10**: 209.
16. Stewart JJP. *J. Comp. Chem.* 1989; **10**: 221.
17. Hay PJ, Wadt WR. *J. Chem. Phys.* 1985; **82**: 270.
18. Wadt WR, Hay PJ. *J. Chem. Phys.* 1985; **82**: 284.
19. Hay PJ, Wadt WR. *J. Chem. Phys.* 1985; **82**: 299.
20. Scrocco E, Tomasi J. In *Advances in Quantum Chemistry*. vol. 11, Löwdin PO (ed.). Academic Press, New York, 1978; 115–193.
21. Frisch MJ, Trucks GW, Schlegel HB, Scuseria GE, Robb MA, Cheeseman JR, Zakrzewski VG, Montgomery Jr JA, Stratmann RE, Burant JC, Dapprich S, Millam JM, Daniels AD, Kudin KN, Strain MC, Farkas O, Tomasi J, Barone V, Cossi M, Cammi R, Mennucci B, Pomelli C, Adamo C, Clifford S, Ochterski J, Petersson GA, Ayala PY, Cui Q, Morokuma K, Malick DK, Rabuck AD, Raghavachari K, Foresman JB, Cioslowski J, Ortiz JV, Baboul AG, Stefanov BB, Liu G, Liashenko A, Piskorz P, Komaromi I, Gomperts R, Martin RL, Fox DJ, Keith T, Al-Laham MA, Peng CY, Nanayakkara A, Gonzalez C, Challacombe M, Gill PMW, Johnson B, Chen W, Wong MW, Andres JL, Gonzalez C, Head-Gordon M, Replogle ES, Pople JA. Gaussian 98, Revision A.7. Gaussian, Inc., Pittsburgh, PA, 1998.
22. Barbieri R, Huber F, Pellerito L, Ruisi G, Silvestri A. In *Chemistry of Tin*, Smith PJ (ed.). Blackie Academic & Professional, London, 1998; 496–540.
23. Fiao XD, Huang FW, Fi LN, Luo BS, Chen LR. *J. Inorg. Biochem.* 1997; **65**: 229.
24. Ivanca MA, Lappin AG, Scheidt WR. *Inorg. Chem.* 1991; **30**: 711.
25. Smith G, Arnold DP, Kennard CHL, Mak TCW. *Polyhedron* 1991; **10**: 509.
26. Pellerito C, Fiore T, Scopelliti M, Di Stefano R, Duca D, Pellerito L. In preparation.
27. van Duijneveldt FB, van Duijneveldt-van de Rijdt JGCM, van Lenthe JH. *Chem. Rev.* 1994; **94**: 1873.
28. Mirisola MG, Pellerito A, Fiore T, Stocco GC, Pellerito L, Cestelli A, Di Liegro I. *Appl. Organomet. Chem.* 1997; **11**: 499.
29. Pellerito L, Maggio F, Fiore T, Pellerito A. *Appl. Organomet. Chem.* 1996; **10**: 393.